Synthesis, Characterization and Adsorptive Properties of Activated Carbon/KFeP₂O₇ Composite

Eduardo Ordoñez Regil[1], Ana Paola Enríquez Sánchez[2], Nidia García González[2], María Guadalupe Almazán Torres[*,1]

[1]Departamento de Química, Instituto Nacional de Investigaciones Nucleares, Carretera México-Toluca, s/n, La marquesa, Ocoyoacac C.P. 52750, Edo. México, México.
[2]Departamento de Ingeniería Química. Tecnológico de Estudios Superiores de Jocotitlán, Carretera Toluca-Atlacomulco km 44.8 Jocotitlán, Edo. México, México.

*Corresponding author:** María Guadalupe Almazán Torres, email: guadalupe.almazan@inin.gob.mx

Abstract. This work deals with the synthesis of nanoparticles of iron-potassium diphosphate, KFeP₂O₇, implanted on activated carbon produced from corncob debris. The chemical composition and structure of activated carbon/potassium-iron diphosphate (AC/KFP) composite was analyzed by X-ray diffraction (XRD), Scanning Electron Microscopy (SEM) and Transmission Electron Microscopy (TEM). Complementary tests were conducted to determine surface characteristics such as surface area and point of zero charge (pH$_{pzc}$). Further, the acid-base titration enabled to determine the surface sites density of AC/KFP composite. Adsorptive properties of AC/KFP composite vis à vis U(VI) was then tested using the batch method.
Keywords: Activated carbon; potassium-iron diphosphate; composite; adsorptive properties.

Resumen. Este trabajo presenta la síntesis de nanopartículas de difosfato de potasio-hierro, KFeP₂O₇, implantadas sobre carbón activado preparado a partir de restos de olote de maíz. La composición química y la estructura del compósito de carbono activado/difosfato de potasio-hierro (AC/KFP) se analizó mediante Difracción de Rayos X, Microscopía Electrónica de Barrido y Microscopía Electrónica de Transmisión. Se realizaron pruebas complementarias para determinar las características de la superficie, como el área de la superficie y el punto de carga cero (pHpzc). Además, la valoración ácido-base permitió determinar la densidad de sitios de superficie del compósito AC/KFP. Adicionalmente, las propiedades adsortivas del compósito AC/KFP frente a U (VI) fueron evaluadas utilizando el método de lotes.
Palabras clave: Carbón activado; difosfato de potasio-hierro; compósito; propiedades adsortivas.

Introduction

Heavy metals represent a risk due to its accumulation in the environment and migration through the water bodies and soils [1]. Removal of these contaminants from wastewater using adsorbent materials has been a viable and effective option.

Several materials have been studied as adsorbents of toxic metal. The first studies conducted on natural materials included clay minerals and carbon-based products [2]. In particular, activated carbon has been widely used as effective adsorbent in environmental applications due to its high porosity and low cost. In addition, chemically modified carbon surface has been found to improve contaminant removal from wastewater [3].

Synthetic reactive compounds have been developed and tested in order to capture specific contaminants. For example, iron compounds, mainly oxyhydroxides and phosphates, have proved their efficiency in capturing heavy metals in solution [4,5].

Recent studies have showed that if the particle size of iron compounds is reduced, the reactivity towards toxic metals is increased. Due to their characteristics that make them highly reactive to specific substances, nanoparticles have been used for wastewater treatment. In fact, this process maximizes its effectiveness by increasing the accessibility to the surface of materials. In this way, the final products require a lower microparticle load, reducing the cost of their use [6]. However, its application requires the use of advanced technologies due to the minute size of the particles, then the identification of an effective and easy to apply technology is vital to be implemented on a large scale. One of the simplest ways of producing nanoparticles is the concomitant synthesis on a sufficiently rigid matrix, durable and manageable size [7]. The choice of the chemical characteristics of nanoparticles is crucial for removing a specific contaminant. Metals or their salts, which have intrinsic catalytic activity, have been successfully used to remove specific undesirable contaminants. For instance, iron and their salts are very effective to remove cationic species when they are in so low concentrations as to become recalcitrant with respect to usual decontamination treatments [8-10].

In general, phosphate compound has shown good efficiency for the retention of U (VI) [11-14]. However, the use of these compounds requires high loads of material to achieve a highly reactive surface toward specific substances. The studies on metal cation adsorption onto nanoparticles of phosphate compound are recent. $KFeP_2O_7$ nanoparticles were successfully synthesized on silica gel beads and used for Cd^{2+} adsorption from an aqueous solution [15,16]. Given the high reactivity of the iron-potassium diphosphate nanoparticles, low concentrations of contaminant react with the high surface area of these particles and remain there.

In order to evaluate other substrates where nanoparticles can be implanted and their high adsorbent capacity can be used, in this work, iron-potassium diphosphate nanoparticles supported on activated carbon $(AC/KFeP_2O_7)$ have been synthetized and proved as an adsorbent to remove toxic metals. Both, carbon and iron-potassium diphosphate, can adsorb anions and cations in solution, separately. The synthesis of a consortium that contains both compounds, can improve the uptake of a wide range of contaminants in solution.

Experimental

Synthesis of AC/ $KFeP_2O_7$ composite

The $AC/KFeP_2O_7$ composite is formed by 2 phases, activated carbon used as substrate and the $KFeP_2O_7$ nanoparticles. Activated carbon was produced from corncob debris. The corncob was fragmented into pieces and boiled for 2 hours using a ratio of 50 % matter and 75% volume of distilled water, in order to remove impurities and lignin. The corncob pieces were dried in a heating system by a light bulb, at a constant temperature of 80 °C for 24 hours, and then reduced to a homogenous powder of 200 mesh. The $AC/KFeP_2O_7$ composite was obtained by pyrolysis process using a tube-type furnace with a Vitro-type Vycor tube resistant to high temperatures (Fig. 1). The corncob powder was incorporated at 10 % wt. to a mixture of $NH_4H_2PO_4$ + $FeCl_3$ in a mortar, adding 10 mL of a KOH 5M solution [17]. This mixture was calcined in the tubular furnace at 300 ˚C for 4 h, under a continuous flow of water saturated nitrogen. After the completion of this stage, the material was washed with abundant distilled water until a constant pH was attained. As a control, activated carbon was prepared from the corncob debris by pyrolysis, using the same conditions for obtaining the $AC/KFeP_2O_7$ composite. Both, activated carbon and the $AC/KFeP_2O_7$ composite, called also as AC/KFP, were subjected to physical-chemical characterization as describe in the next section.
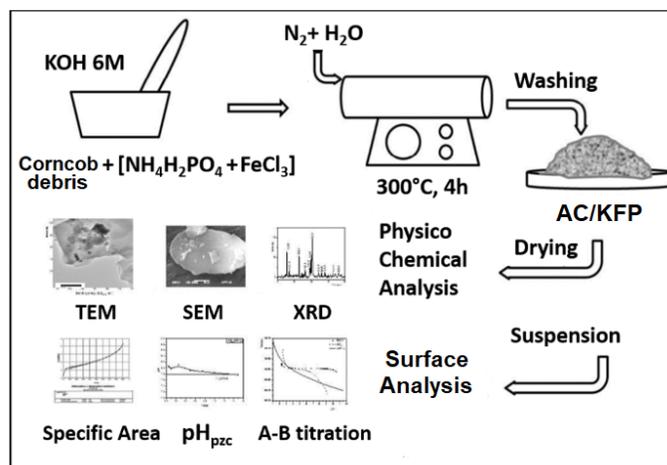
Fig. 1. Experimental setup for synthesis of Activated Carbon/ $KFeP_2O_7$ composite.

Physicochemical characterization

The synthesized materials were characterized by different analytical techniques, including X-ray Diffraction (XRD), Scanning Electron Microscopy (SEM) and Transmission Electron Microscopy (TEM). XRD patterns of AC/KFP were obtained by means of a diffractometer D-5000 Siemens using a copper anode (λ = 1.543 Å). The Kα radiation was selected with a diffracted beam monochromatic. The XRD peaks were measured in the 2θ range from 4° to 70°, the resulting patterns were compared whit those reported in the JCPDS.

The morphology of activated carbon and $KFeP_2O_7$ nanoparticles were observed by means of Scanning Electron Microscopy (SEM) at various magnification rates. Energy Dispersion Spectroscopy (EDS) microprobe coupled to the SEM device was used to determine the elemental chemical composition of samples. SEM micrographs were obtained on a JEOL 5900LV scanning electron microscope at 25 kV. Samples were mounted on a stub of aluminum with carbon tape and later covered with a gold layer, approximately 150 Å thick, using a Denton Vacuum Desk II platter. In all cases, the images were obtained using a backscattered electron detector. The elemental chemical composition of samples was determined through EDS on an EDAX-4 spectrometer.

Transmission electron microscopy (TEM), in bright and dark field modes, was performed to obtain structural images of AC/KFP composite. Transmission electron microscopy studies were performed to have a powerful approximation of sample surface using a microscope JEOL 2010 operating at 200 kV. Elemental analysis was carried out by Energy Dispersive X-ray (EDX) spectrometry. Sample was prepared by dissolving it with a mixture of $(CH_3)_2SO/CH_3CN$ (1:1) using an ultrasonic bath and then suspended in acetone and placed on a copper grid.

Surface characterization

The surface properties of the studied materials have been determined as follows: surface area was measured by N_2 Brunauer-Emmett-Teller (BET) method on a Micromeritics Gemini 2360 surface area analyzer. The sample was first degassed to remove gases and vapors that may have become physically adsorbed onto solid surface during handling, and then analyzed applying a multi-point N_2 adsorption-desorption method.

The point of zero charge (pH_{pzc}) is described as the pH at which the surface has a net neutral charge. The pH_{pzc} value was determined by mass titration experiments according to the experimental procedure described by Noh and Schwartz [18, 19]. Different amounts of AC/KFP were weighed in 0.01, 0.05, 0.1, 0.2, 0.5, 1.0, 1.5 and 2 g batches and placed in polypropylene tubes containing 10 mL of water. The resulting suspension was kept under agitation for 24 h and then centrifuged at 3500 rpm for 15 min. The pH values of the liquid supernatants were then measured and plotted as a function of % mass.

The acid-base properties of materials were determined by potentiometric titration experiments [20]. Potentiometric titrations are performed using a Radiometer Titralab 90 attached to an ABU901 autoburte. Aqueous suspensions of 0.1 g of activated carbon or AC/KFP composite in 30 mL 0.5 M $NaClO_4$ solution were prepared and adjusted to pH 2.0. After pH equilibration, suspensions were titrated with 0.1M NaOH solution under a nitrogen-controlled atmosphere using an Ag/AgCl electrode. During the experiments, the suspension was stirred continuously to prevent settling of the suspension and promote reaction with the titrant solution.

Sorption experiments

Adsorptive properties of AC/KFP composite were studied by means of sorption experiments using the conventional batch method. Suspensions with 100 mg of AC/KFP composite and 10 mL of 0.5 M $NaClO_4$ solution were prepared and agitated for 24 h at room temperature under nitrogen atmosphere. The suspensions were centrifuged, and the remaining solution separated and replaced with 10 mL of 1×10^{-2} M $UO_2(NO_3)_2$ solution and agitated again for 24 h. Final pH values were then measured and the uranium concentration quantified by liquid scintillation method using a TRI-CARB 2700TR PACKARD Liquid Scintillation Analyzer.

Results and Discussion

Synthesis of AC/ KFP composite

The synthesized material was an easy-to-handle condensed phase without volatile particles. After pyrolysis, the material was gently milled and sieved to homogenize the particles, then rinsed several times in order to ensure the absence of unreacted chemicals.

Physicochemical characterization

Synthetized material was evaluated by suitable physical and chemical analyses. XRD pattern of sample shows the characteristic $KFeP_2O_7$ signals (PDF chart 00-036-1457), while activated carbon is observed as a continuous amorphous signal (Fig. 2**(a)**), although it exhibits some crystallinity, which is in good agreement with the carbon standard card (00-044-0558 PDF). This can be explained because under our preparation conditions, part of carbon crystallizes in the form of graphite. The structure of $KFeP_2O_7$ was represented as a three-dimensional single crystal of monoclinic symmetry of the P 21/c space group whose cell parameters were: a = 7.352; b = 9.987; c = 8.187 Å, β = 106.49º, corresponding to a low temperature form. The adaptation of the diphosphate groups $[P_2O_7]$ to the octahedral $[FeO_4]$ framework and the layered disposition of tetrahedra and octahedra lead to the formation of tunnels (Fig. 2**(c)**). The result is a cage structure where the potassium atoms within the framework can be replaced with similar atoms by means of a cationic exchange process. This structure was subjected to an XRD modeling on the basis of the CaRIne v3.2 Crystallography package. The result was very close to the experimental diffraction pattern (Fig 2**(b)**) [21-22].

SEM images at 250x and 1700x magnifications for activated carbon are shown in Fig. 3. Activated carbon from corncob debris present a porous texture with small irregular cavities (Fig. 3**(a)**). It can be also observed that the material preserves its original structure and relative rigidity (Fig. 3**(b)**). The elemental chemical composition determined by Energy Dispersive Spectroscopy (EDS) confirms the presence of carbon (87.41 %), oxygen (11.37 %) and a lower concentration of potassium (1.20 %). The unmarked peak corresponds to the gold deposited to confer conductivity to the sample (Fig. 3**(c)**).

The deposition of $KFeP_2O_7$ particles on the activated carbon was also corroborated by SEM analysis. SEM micrographs at 10000x and 50000x magnifications are shown in Fig. 4. $KFeP_2O_7$ particles with spherical shape and sizes ranging from 90 and 100 nm are observed in Fig. 4**(b)**. These particles cover a large surface area of the activated carbon, including its cavities. It should be noted that synthesis in reduction conditions over organic matter prevents the formation of agglomerates limiting the growth of potassium iron diphosphate particles during the pyrolysis process [23]. In addition to the reducing conditions, the presence of inert gas during synthesis promote the formation of small $KFeP_2O_7$ particles homogeneously distributed on activated carbon. Elemental chemical composition of AC/KFP determined by Energy Dispersive Spectroscopy (EDS) confirms the presence of C (86.41 %), O (11.35 %), P (1.23 %), K (1.72 %) and Fe (0.86 %).
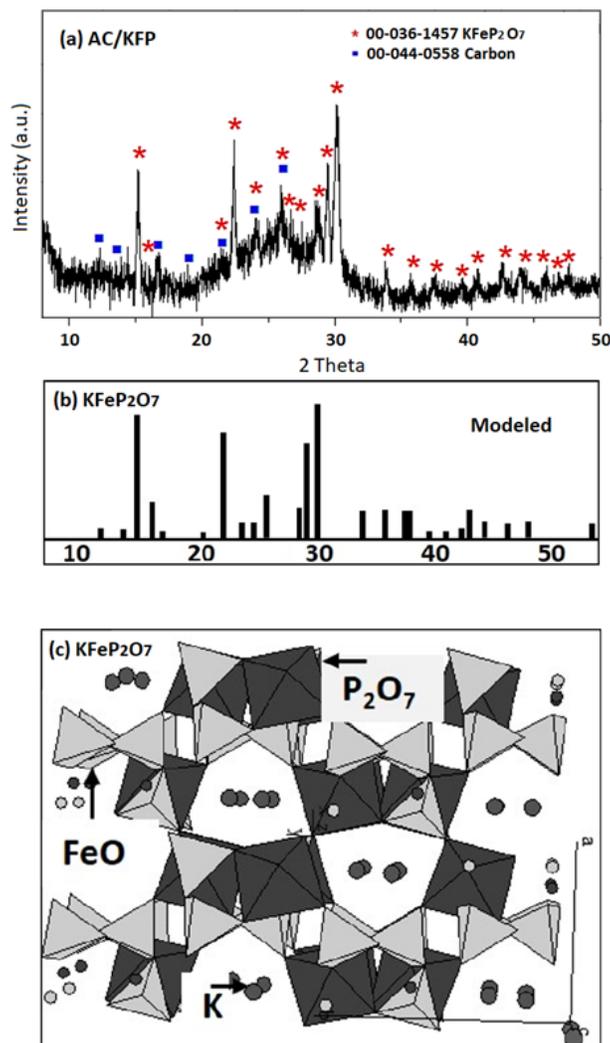
Fig. 2. (a) AC/KFP composite diffraction pattern, **(b)** modeled KFeP$_2$O$_7$ diffraction pattern, **(c)** modeled KFeP$_2$O$_7$ structure.
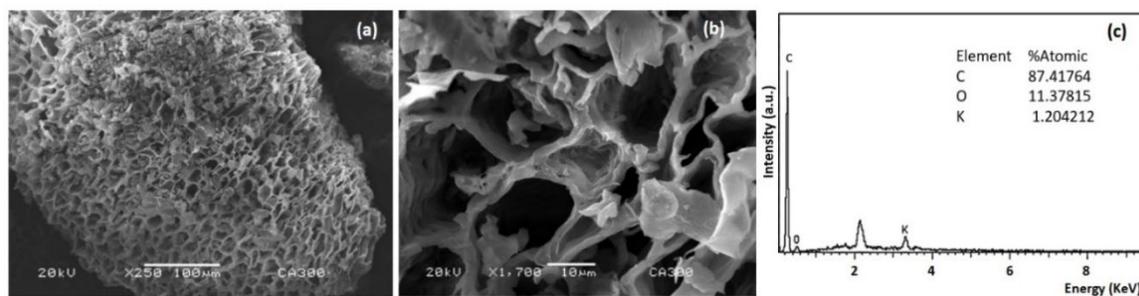
Fig. 3. SEM micrographs of activated carbon at **(a)** 250x and **(b)** 1700x magnifications, **(c)** EDS elemental analysis.
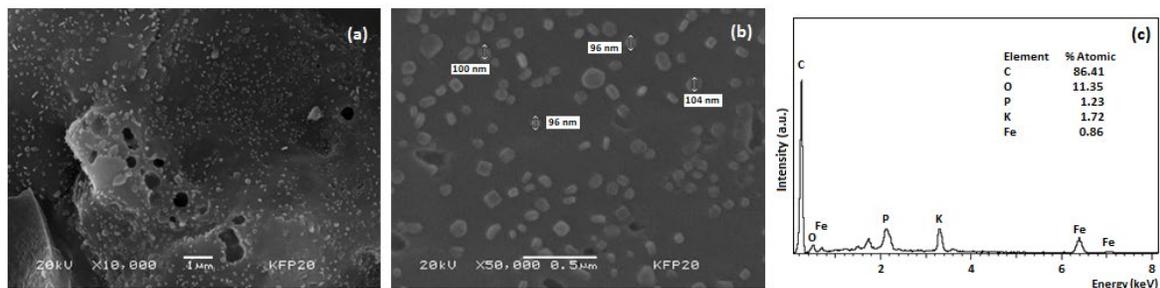
Fig. 4. SEM micrographs of AC/ KFP composite at **(a)** 10000x, **(b)** 50000x magnifications, **(c)** EDS elemental analysis.

TEM images of AC/KFP composite obtained after the pyrolysis process are presented in Fig. 5. In Fig. 5**(a)**, activated carbon is observed as laminar translucent forms [24, 25] and on these small dark forms of greater density, whose size is in the order of nanometers are associated to the KFP particles. These results agree with those of SEM analysis, where $KFeP_2O_7$ is observed as small spherical particles. These results are also consistent with those obtained in previous studies [26-27]. Dark-field mode micrograph shows a section of composite where there was no KFP particles (Fig. 5**(b)**). In this, striated areas are observed that reveal graphite-type atomic arrangements. In Fig. 5**(c)**, activated carbon appears as concentric rings which denote an amorphous compound, while $KFeP_2O_7$ particles implanted produces a bright dot pattern. The implantation of nanoparticles over the activated carbon surface is clearly seen and this effect can cover the entire carbon matrix as discussed in the XRD section.
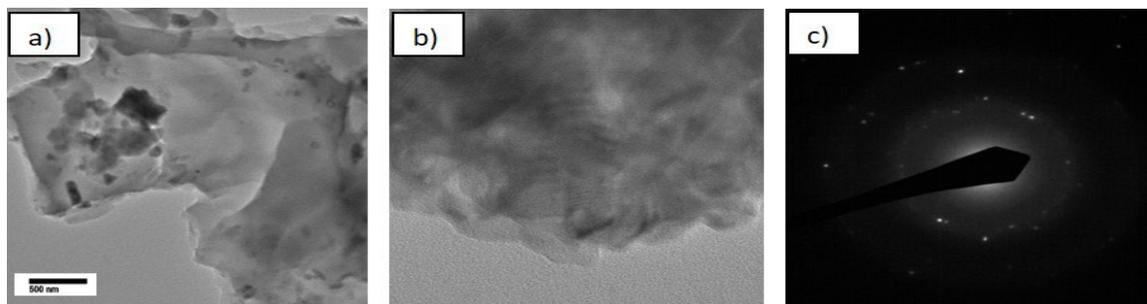
Fig. 5. TEM images of AC/KFP composite: **(a)** bright field, **(b)** dark field, **(c)** $KFeP_2O_7$ diffraction pattern.

Surface analysis

The surface parameters of activated carbon and AC/KFP composite are summarized in Table 1. The specific surface area (BET) for both, activated carbon and AC/KFP composite, were found to be 1.497 m²/g and 2.436 m²/g, respectively. This increase in the surface area value can certainly be attributed to the implantation of microspheres on activated carbon surface.

Table 1. Surface parameters for Carbon and AC/KFP composite.

Materials	Activated Carbon	AC/KFP
Specific surface area (BET)	1.497(m²/g)	2.436(m²/g)
Point of zero charge (pH_{pzc})	8.2	8.4
Surface Site Density (δs)	5.80E-02 (s/nm²)	6.29E-02 (s/nm²)

The values of point of zero charge (pHpzc), determined by mass titration experiments, were around 8.2±0.2 for both activated carbon and AC/KFP composite. This may be because the amount of KFP microparticles deposited on the activated carbon is too small to have a significant effect on the point of zero charge, which is defined by the substrate (activated carbon). The value of pH_{pzc} obtained is within the range typically reported by several authors for this kind of carbonaceous materials [28]. Finally, surface site density value for AC/KFP composite is slightly greater than the value obtained for activated carbon (Table 1). This can be explained by the presence of OH-groups created from FeO groups shared with diphosphate layers in the microspheres on activated carbon surface, which does not depend on surface area but rather on intrinsic properties of AC/KFP composite.

Adsorptive properties

Fig. 6**(a)** shows sorption isotherms for U(VI) onto Activated Carbon and AC/KFP composite. For activated carbon, U(VI) sorption reaches a maximum (~50 %) at pH 5.3. The sorption of U(VI) onto AC/KFP composite increases significantly reaching a maximum of 78 %. This increase is surely due to the KFeP$_2$O$_7$ micro particles. At low pH's, sorption is mainly due to the presence of the UO_2^{2+} (Fig. 6**(b)**) which reacts with the composite. The solution pH promotes the formation of the UO$_2$(OH)$_2$·H$_2$O (Fig. 6**(b)**) as condensed phase over AC/KFP composite, which precipitate in the less acidic conditions after pH> 4.5. A comprehensive analysis of the sorption properties of AC/KFP composite will be presented in a forthcoming study.
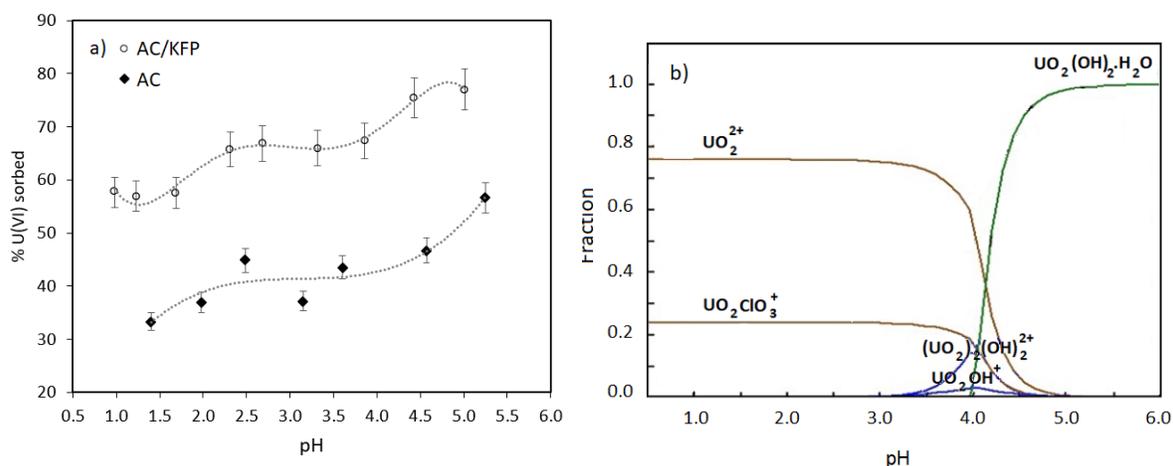
Fig. 6. (a) Sorption isotherms for U(VI) onto Activated Carbon and AC/KFP composite, **(b)** speciation diagram of uranium (VI).

Conclusion

An improved method for synthesis of KFeP$_2$O$_7$ nanoparticles implanted on activated carbon was achieved successfully. Several analytical techniques have shown that KFeP$_2$O$_7$ particles are microspheres homogenously distributed throughout the surface of activated carbon produced from corncob debris.

The implanted KFeP$_2$O$_7$ nanoparticles enhance the adsorptive properties of activated carbon vis-a-vis uranium. The surface area is larger and can provide a high sorption capacity for cations in solution. It was noticed that after the sorption process, KFeP$_2$O$_7$ nanoparticles were maintained at the surface of activated carbon. Furthermore, the size and shape of AC/KFP composite make it easy to handle and kept a high reactivity over a wide pH range.

Acknowledgments

References

1. González, J. *J. Agric. Res.* **2007**, *68*, 56-68.
2. Robinson, S. M.; Parrott Jr., J. R. Technical Report, 1989, ORNL/ TM-10836.
3. De la Rosa-Gómez, I.; Olguín, M. T.; Alcántara, D. *J. Mex. Chem. Soc*. **2010**, *54*, 139-142.
4. Granados-Correa, F.; Corral-Capulin, N. G.; Olguin, M. T.; Acosta-Leon, C. A. *Chem. Eng. J.* **2011**, *171*, 1027-1034. DOI: 10.1016/j.cej.2011.04.055.
5. Granados-Correa, F.; Serrano-Gomez, J. *J. Chil. Chem. Soc.* **2010**, *3*, 283-287.
6. Kreuter, J. *Int. J. Pharm.* **2007**, *331*, 1-10.
7. Barrena, R.; Casals, E.; Colón, J.; Font, X.; Sánchez, A.; Puntes, V. *Chemosphere.* **2009**, *75*, 850-857. DOI: 10.1016/j.chemosphere.2009.01.078.
8. Mathialagan, T.; Viraraghavan, T. *Sep. Sci. Technol.* **2003**, *38*, 57-76. DOI:10.1081/SS-120016698.
9. Sasakia, K.; Nakano, H.; Wilopo, W.; Miura, Y.; Hirajima, T. *Colloids Surf, A Physicochem. Eng. Asp.* **2009**, *347*, 8-17. DOI: 10.1016/j.colsurfa.2008.10.033
10. De Dios, A. S.; Díaz-García, M. E. *Anal. Chim. Acta.* **2010**, *666*, 1-22. DOI:10.1016/j.aca.x2010.03.038.
11. Drot, R.; Lindecker, C.; Fourest, B.; Simoni, E. *New J. Chem.* **1998**, *22*, 1105-1109.
12. Ordoñez-Regil, E.; Drot, R.; Simoni, E.; Ehrhardt, J.J. *Langmuir.* **2002**, *18*, 977-7984
13. Finck, N.; Drot, R.; Lagarde, G.; Mercier-Bion, F.; Catallete, H.; Simoni. E. *Radiochim. Acta*. **2008**, *96*, 11-21
14. Almazan-Torres, M.G.; Drot, R.; Mercier-Bion, F.; Catalette, H., Den Auwer, C.; Simoni, E. *J. Colloid Interface Sci.* **2008**, *323*, 42-51.
15. Ordoñez-Regil, Ed.; Ordoñez-Regil, En.; García-González, N.; Barocio, *Am. J. Anal, Chem.* **2012**, *3*, 512-517.
16. Ordoñez-Regil, Ed.; Granados-Correa, F; Ordoñez-Regil, En.; Almazán-Torres, M. G. *Environ. Technol*. **2015**, *36*, 188-197.
17. Alfonso, B. F.; Blanco, J. A.; Fernández-Díaz, M. T.; Trobajo, C.; Khainakov S. A.; García, J. R. *Dalton Trans.* **2010**, *39*, 1791-1796. DOI:10.1039/b912427f.
18. Huang, J. W.; Su, P.; Wu, W. W.; Wu, X. H. *App. Chem. Ind.* **2011**, *40*.
19. Noh, J. S.; Schwartz, J. A. *J. Colloid Interface Sci.* **1989**, *130*, 157-164. DOI:10.1016/0021-9797(89)90086-6.
20. Bell, L. C.; Posner, A. M.; Quirk, J. B. *J. Colloid Interface Sci.* **1973**, *42*, 250-256. DOI:10.1016/0021-9797(73)90288-9.
21. Gabelica-Robert, M.; Goreaud, M.; Labbe, Ph.; Raveau, B. *J. Solid State Chem.* **1982**, *45*, 389-395. DOI:10.1016/0022-4596(82)90184-0.
22. Riou, D.; Labbe, P.; Goreaud, M. *Rev. Chim. Miner.* **1988**, *25*, 215-229.
23. Ordoñez-Regil, E.; Granados-Correa, F.; Ordoñez-Regil, Ed.; Almazán-Torres, M. G. *Environ. Technol.* **2015**, *36*, 188-197.
24. Bonet, M.; Quijada, C.; Cases, F. *Can. J. Anal. Sci. Spect.* **2004**, *49*, 234-239.
25. Alcañiz-Monge, J.; Blanco, C.; Linares-Solano, A.; Brydson, R.; Rand, B. *Carbon.* **2002**, *40*, 541-550.
26. Zhang, Y.; Chen, Y.; Westerhoff, P.; Hristovski, K.; Crittenden, J.C. *Water Res.* **2008**, *42*, 2204-2212.
27. Ma, H. ; Qi, X. ; Maitani, Y. ; Nagai, T. *Int. J. Pharm.* **2007**, *333*, 177-186.
28. Sun, Y. P.; Li, X.Q.; Zhang, W. X.; Wang, H.P. *Colloids Surf. A Physicochem. Eng. Asp.* **2007**, *308*, 60-66.